Soft Matter

Cite this: *Soft Matter*, 2012, **8**, 10853

www.rsc.org/softmatter

PAPER

Soft biodegradable polymersomes from caprolactone-derived polymers†

Joshua S. Katz,‡[a] Katherine A. Eisenbrown,[a] Eric D. Johnston,[a] Neha P. Kamat,[a] Jeff Rawson,[b] Michael J. Therien,[b] Jason A. Burdick[a] and Daniel A. Hammer*[ac]

Received 1st June 2012, Accepted 3rd August 2012
DOI: 10.1039/c2sm26275d

Polymersomes have promise for advanced theranostic delivery. We report here the design and characterization of a series of block copolymers that assemble into soft, bioresorbable, and non-toxic vesicles. The polymers are based on poly(ethylene glycol)–poly(caprolactone), but the caprolactone (CL) is copolymerized with a second monomer, 1,4,8-trioxaspiro-[4,6]-9-undecanone (TOSUO). Because TOSUO polymers have no crystalline character, copolymerizing TOSUO with CL should reduce the crystallinity of the polymersomes. After synthesizing polymers with different ratios of CL to TOSUO, we found that all copolymers assemble into both micron and nano-metric vesicles. Increasing the TOSUO content of the copolymer reduces the polymer crystalline melting temperature and the area expansion modulus of vesicle membranes. Membranes with partial crystalline structure exhibit hysteresis in the tension *versus* strain curve during aspiration. Vesicles are not cytotoxic and exhibit first-order release of encapsulated gemcitabine. These materials are promising for the development of deformable, biodegradable polymersomes for biomedical applications.

Introduction

A major limitation to current treatments for many diseases is the inability to adequately deliver diagnostics and therapeutics in sufficient quantity directly to the site of disease.[1] To address these issues, a variety of polymer-based systems have been explored to improve *in vivo* biodistribution and better protect the encapsulants from harsh biological conditions. One vehicle that is particularly attractive for encapsulation of such materials is the polymer vesicle or polymersome.[2,3] Self-assembled from block copolymers and similar in structure to liposomes, polymersomes have the ability to simultaneously encapsulate large quantities of both hydrophilic and hydrophobic materials, allowing encapsulation efficiencies and quantities similar to liposomes for hydrophilic materials and solid particles (*i.e.* micelles, nanoparticles) for hydrophobic materials in tandem.[3] As a result of their block copolymer membrane, they additionally have superior mechanical stability compared to their lipid counterparts and, when constructed from poly(ethylene oxide) (PEG) hydrophilic blocks, the resulting polymersomes resist opsonization.[4]

Since their initial design, the re-engineering of polymersomes has increased their usefulness for biomedical applications.[5] Ahmed and coworkers demonstrated the dual delivery of hydrophobic and hydrophilic drugs, paclitaxel and doxorubicin, respectively, using a single vesicle formulation by blending degradable and non-biodegradable polymers.[4] Near IR-emissive polymersomes, whose membranes are loaded with large hydrophobic porphyrin dyes,[6] have shown potential for *in vivo* imaging; demonstrated applications include locating tumors or the tracking of dendritic cells.[7,8] Numerous groups have explored the attachment of targeting ligands to the surface of polymersomes to enhance their uptake and binding to specific cells in both *in vitro* and *in vivo* environments, and some studies have indicated that such peptides influence polymersome assembly.[9–14] However, a limitation of these studies is that with few exceptions,[10] much of this work has been accomplished with non-biodegradable vesicles.

Several approaches have also been explored to alter the dynamics of release of encapsulated agents, including post-assembly membrane polymerization and the introduction of UV-sensitive groups that allow the release of contents upon exposure to UV light.[15–21] In a recent example, Hammer and coworkers developed a composite system in which polymersomes containing membrane-loaded, NIR-emissive porphyrin-based fluorophores and aqueously encapsulated protein or high molecular weight dextran became photo-sensitive.[16,18] These vesicles, when exposed to visible light within the porphyrin excitation bands, underwent spontaneous disassembly and collapse, leading to contents release. Studies demonstrated that sensitivity of response of the parent vesicle could be tuned by the molecular

[a]*Department of Bioengineering, University of Pennsylvania, 210 S. 33rd Street, 240 Skirkanich Hall, Philadelphia, PA 19104, USA. E-mail: hammer@seas.upenn.edu*
[b]*Department of Chemistry, Duke University, Durham, NC 27708, USA*
[c]*Department of Chemical and Biomolecular Engineering, University of Pennsylvania, Philadelphia, PA 19104, USA*

† Electronic supplementary information (ESI) available. See DOI: 10.1039/c2sm26275d

‡ Present address: Formulation Science, The Dow Chemical Company, Spring House, PA 19477, USA.

weight of the polymer itself; higher molecular weight polymers led to thicker, more robust membranes that were less sensitive to photorelease.[16]

While many advances have been made in the development of biocompatible polymersomes that may be useful for medical applications, a major limitation is in the polymers themselves. Polymersomes assembled from hydrophobic blocks of poly(ethylethylene) or poly(butadiene) are unlikely to gain regulatory approval for use in humans because of their inability to be degraded or cleared. Thus, more attention needs to be paid to polymer synthesis. Battaglia and coworkers developed diblock copolymers that became fully water soluble at endosomal pH, leading to polymersome disassembly,[22–24] but these polymers could reprecipitate at neutral pH before clearance. As an alternative, several groups have synthesized polymersomes based on hydrolytically degradable polymers, such as poly(caprolactone) (PCL),[25] poly(lactide),[26] or poly(trimethylene carbonate).[27] These polymers have already been approved for biomedical applications. We recently reported vesicles made solely from PEG–PCL,[25] and then later articulated a route to preparing bioresorbable PEG–PCL polymers that allow for UV-induced cleavage of the PEG, triggering contents release.[20] However, poly(caprolactone) has a high crystalline melting temperature, and PEG–PCL leads to the formation of polymersomes with solid rather than fluid membranes at room or body temperature.[28] Zupancich and coworkers studied the assembly of a family of non-crystalline poly(methylcaprolactone)–poly(ethylene glycol) amphiphiles of different molecular weights and ethylene glycol block fractions; a subset of these polymers assemble into vesicles, though characterization beyond morphology was not reported.[29]

Fluid membranes have several advantages over solid membranes. It is known that membrane rheology can significantly influence how polymersomes interact with their surroundings.[13] A fluid membrane enables increased contact area between a vesicle and substrate as the vesicle can deform and flatten on a surface. In contrast, solid membranes can only interact with a substrate through a smaller contact area as no conformational change can occur to improve the contact area. Additionally, fluidity in a membrane allows for diffusion of ligands, allowing for the formation of clusters, further enhancing binding.[30,31] Consequently, binding between fluid vesicles and a substrate (*i.e.* components of a tissue) would be enhanced compared to a solid vesicle's binding.[32,33] Another advantage of fluid membrane vesicles is their ability to bend and deform through small spaces *in vivo*. The typical "leaky junction" in tumor vasculature has a diameter of 40–80 nm, which is smaller than the typical polymersome diameter.[34] Consequently, to successfully passivate tumor tissue, vesicles would have to deform, by elongating, to fit through the endothelial pore.[35] Such behavior could only be exhibited in fluid membrane vesicles. Finally, crystallinity implies association of polymers into multimolecular aggregates. If the degradation rate of each element of the aggregate is sufficiently slow, these aggregates could lodge undesirably in cells and kidneys as crystalline aggregates.

Recognizing the need to develop fluid, flexible membranes from non-toxic, biodegradable polymers, we report here the design and characterization of vesicles assembled from a series of diblock copolymers. To form these copolymers, we copolymerized caprolactone (CL) with a second monomer, 1,4,8-trioxaspiro-[4,6]-9-undecanone (TOSUO), that has no crystalline character in polymer form.[36–38] TOSUO was originally developed as a protected form of γ-hydroxycaprolactone that could undergo controlled ring-opening polymerization.[36,38] While such a material, containing degradable ester linkages with modifiable alcohol side chains, is highly promising for many biomedical applications, there has been only one report of its use, and only as the protected form.[39] Wang and coworkers designed solid nanoparticles comprised of copolymers of TOSUO and CL. In their work, they found minimal cell cytotoxicity, indicating that polymers containing TOSUO could be useful as biomaterials. Seeing the promise in this material, we chose to investigate it as a potential route to developing soft biodegradable polymersome membranes. We synthesized a series of block copolymers of PEG with copolymerized TOSUO/CL and characterized their chemical and thermal properties in bulk. All copolymers robustly assembled into both micron-sized and nano-sized vesicles. These vesicles were characterized for their mechanical rigidity, cytocompatability, and membrane transport properties.

Results and discussion

Polymer characterization

All polymers were synthesized by the transition-metal catalyzed ring opening polymerization of the cyclic lactone(s) using monomethoxy-PEG as a macroinitiator (Scheme 1). Prior reports have indicated that caprolactone and TOSUO polymerize at roughly the same rate, and therefore, random copolymerization of that block occurs.[37] In total, 4 amphiphiles were synthesized (Table 1), one in which the hydrophobic block was synthesized solely from CL (PCL), one in which it was synthesized solely from TOSUO (PTS), and two with different ratios of CL to TOSUO : CT31 has a 3 : 1 molar feed ratio while CT21 has a 2 : 1 molar feed ratio. All polymers have the same 2 kDa hydrophilic PEG block. Polymer composition and degree of polymerization were analyzed by proton NMR and all closely matched their feeds and target molecular weights (Fig. S1†). Additionally, all polymers had low polydispersity indices (~1.1 to 1.2 as determined by gel permeation chromatography), a characteristic necessary for spontaneous membrane assembly.[40]

We characterized the polymers for their thermal properties by differential scanning calorimetry (DSC) (Fig. 1). As expected, the polymers exhibited composition-dependent glass transition

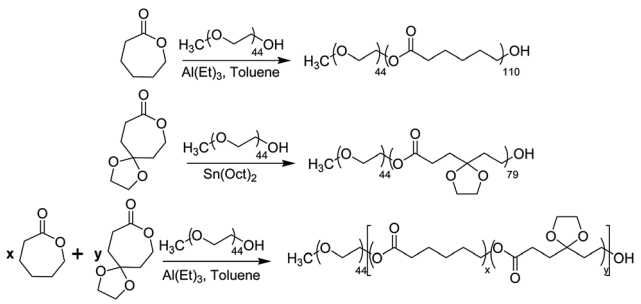

Scheme 1 Synthesis of PCL (top), PTS (middle), and CT21 and CT31 (bottom). For CT21, $x,y = 64,36$; for CT31, $x,y = 77,23$.

Table 1 Chemical and physical characterization of diblock copolymers

Name	CL/TOSUO feed ratio [molar]	CL/TOSUO calc. ratio [molar][a]	DP[a,b]	M_n [kg mol^{-1}][a]	PDI[c]	T_g [oC][d]	T_m [oC][d]
PCL	100/0	100/0	110	14 540	1.17	−61.3	54.8, 57.4
CT31	75/25	77/23	97	14 290	1.21	−59.1	32.0, 38.3
CT21	67/33	64/36	76	12 147	1.13	−53.0	29.9
PTS	0/100	0/100	79	15 500	1.20	−34.8	n/a[e]

[a] Determined by NMR. [b] Degree of polymerization. [c] Determined by GPC. [d] Determined by DSC. [e] This sample had no crystalline melt.

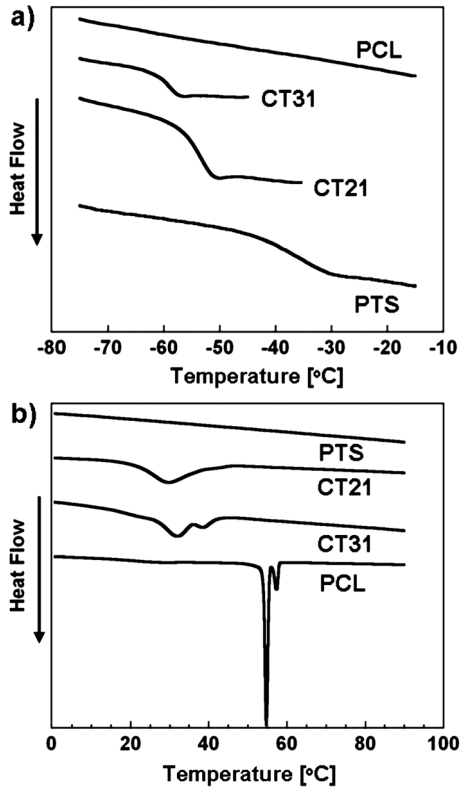

Fig. 1 Differential scanning calorimetry of diblock copolymers. Heat flow curves showing the (a) glass and (b) crystalline melting transitions for the polymers. The scale of the curve in (a) does not allow visualization of the PCL transition at −61.3 °C.

temperatures; all polymers had a glass transition temperature well below room temperature. PTS had the highest glass transition temperature, −34.8 °C, while PCL had the lowest at −61.3 °C. CT31's and CT21's transitions fell between these two, though both significantly closer to that of PCL than PTS (−59.1 and −53.0 °C, respectively). At elevated temperatures, all polymers except for the PTS had marked crystalline melts. Prior reports indicate that above a composition of approximately 15% TOSUO, CL/TOSUO copolymers lose their crystallinity.[37] While we did find crystalline transitions for CT31 and CT21, they were markedly less pronounced than the PCL. CT31, CT21 and PCL all show a double melting peak, likely due to the individual melting of each block of the copolymers (*i.e.* PEG and CL).[29] No PEG melting was observed for the PTS sample, likely due to the TOSUO block disrupting any PEG crystallinity.[39] As the content of TOSUO was increased in the polymer, the melting point decreased from approximately 55 °C (PCL) to 35 °C (CT31) to 30 °C (CT21). Additionally, CT21's melting peak was broad enough that only a single peak temperature (rather than two) could be elucidated. The drop in temperature of the PEG crystalline peak is likely caused by weakening of the crystal by the presence of increasing amounts of TOSUO in the hydrophobic block (which can solubilize the PEG) until no crystal can form as observed for the PTS sample. Consistent with its strong crystallinity, when cooled from 100 to −80 °C at a rate of 5 °C min^{-1}, only the PCL reformed its crystal; the others only reformed when reheated above the glass transition temperature. However, when the rate of cooling was slowed to 1 °C min^{-1}, CT31 did recrystallize. Even at a rate of 0.25 °C min^{-1}, CT21 did not recrystallize during cooling. Thus, we synthesized a group of polymers that exhibit a full range of crystallinity at physiologically relevant temperatures.

Vesicle formation and characterization

Thin films of the polymers were rehydrated with aqueous solution and vesicles spontaneously formed for all four polymers (Fig. 2). To assemble micron-sized (giant) vesicles, following addition of the aqueous media, the films were incubated at 62 °C for 48–72 hours and then vortexed. The hydration procedure precluded blending PCL and PTS as a route to forming hybrid membranes; the incubation temperature (necessary to melt the CL blocks) enabled phase separation of the blended film,[36] leading to a mixed population of PCL vesicles and PTS vesicles rather than a single population of PCL/PTS blended vesicles.§ Confocal microscopy shows the assembly of large vesicles of the four individual polymers. Polymersomes from films that were co-cast with an ethyne-linked zinc porphyrin dimer (**PZn_2**) show membrane-localized fluorescence,[6,8] additionally confirming the membrane structure of the vesicles. Multilamellar vesicles were observed, which is not uncommon for giant vesicles. Additionally, many vesicles were observed with branch-points in the membrane, leading to non-spherical, interconnected, and irregularly shaped vesicles (Fig. S2†). Formation of such structures was unpredictable and they were often found alongside "normal" vesicle morphologies. These morphologies were not observed for PCL vesicles. This behavior could be due to the exact molecular weights of the TOSUO-containing polymers not being the most

§ We qualitatively found within a sample of polymersomes formed from a 50/50 wt/wt blended film of PCL and PTS that some vesicles were rigid and could not be aspirated into a pipette and that others were easily aspirated. Additionally, the films of these blends became opaque upon heating, suggesting micro phase separation of the two polymers. Studies exploring these phenomena are ongoing.

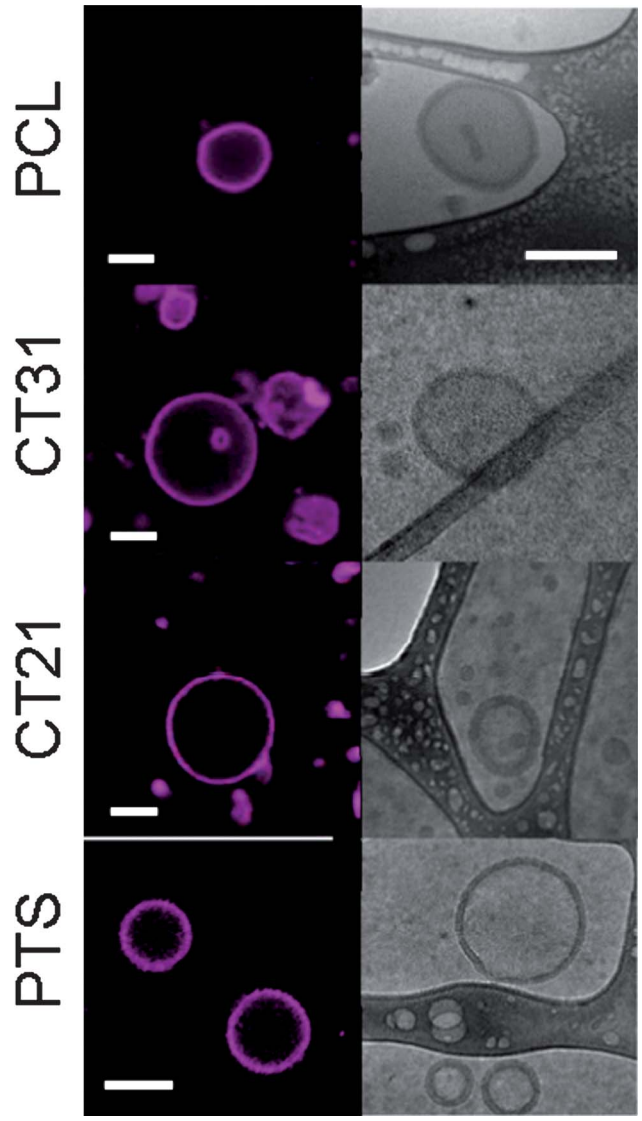

Fig. 2 Images of polymersomes. Polymersomes of PCL, CT31, CT21, and PTS were imaged by (left) confocal microscopy (giant vesicles) and (right) cryoTEM (nano vesicles). The confocal images show $\mathbf{PZn_2}$ fluorescence, localized to the membranes of vesicles. Scale bars are 10 μm for confocal images and 200 nm for cryoTEM images.

ideal for vesicle formation or the substituent ketone in the TOSUO introducing packing instabilities to the membrane. The PCL vesicles appear spherical, though are not as smooth in appearance as the TOSUO-containing vesicles. The smooth nature of the PCL vesicles is likely due to the rapid cooling of the vesicle solution following hydration, locking the vesicle in a spherical shape formed at higher temperature.[29]

Nano-sized[41] vesicles were obtained by sonication of the hydrated films at the same elevated temperature used for simple hydration. To reduce the presence of multilamellar vesicles, we processed the vesicles through 4 freeze/thaw cycles. We found that PTS, CT21 and CT31 vesicles all could be extruded through 200 nm membranes at room temperature (indicating some degree of membrane fluidity), though studies reported in this paper involve non-extruded vesicles. As has been previously reported, PCL vesicles required extrusion at elevated temperatures and under high pressure.[5] This suggests that post-processing of TOSUO-containing vesicles is likely more facile than for PCL vesicles. To examine the morphology of nano vesicles, we utilized cryogenic transmission electron microscopy (cryoTEM). For all samples, robust polymersomes ranging in size from approximately 50 to 400 nm were observed (Fig. 2). A population of cylindrical micelles was also observed on several occasions for the PTS sample (Fig. S3†), but this morphology was not observed in other samples.

Prior *in vitro* studies have suggested that TOSUO-based materials are cytocompatible.[39] To confirm that our formulations are also compatible with cell growth, we performed cell cytocompatibility studies, incubating 3T3 fibroblasts, human mesenchymal stem cells (hMSCs), and human umbilical cord vein endothelial cells (HUVECs) with nano polymersomes (Fig. 3). Following the continuous incubation of vesicles for 24 hours and an additional 24 hours of cell growth, cell activity dropped minimally at polymer concentrations as high as 100 μg mL^{-1}, compared to polymersome-free controls. A slight, but statistically significant, drop in cell activity was observed for CT31 in hMSCs and CT21 in hMSCs and HUVECs at the highest polymersome concentration (100 μg mL^{-1}). This drop could possibly be attributed to the more sensitive nature of these cell lines, lower polymer tolerance, or perhaps trace impurities in the material. Direct extrapolation of this data to *in vivo* behavior should not be inferred, as the *in vivo* nature of organisms is quite different from isolated cells cultured in two dimensions. However, this data in total indicates that the CL/TOSUO copolymers are indeed promising for further exploration as biocompatible, biodegradable soft materials.

Membrane mechanics

Much of this work was guided by the hypothesis that fluid, flexible membranes are superior to solid membranes for applications in *in vivo* drug delivery and imaging. Indeed, prior studies have indicated that membrane rheology can significantly affect the interaction and binding of vesicles with ligand-bearing substrates.[13] We used micropipette aspiration to probe the rheological properties of giant polymersomes. As has been previously reported, we found that PCL vesicle membranes are solid and are unable to be aspirated.[25,28] Vesicles from PTS, CT21 and CT31 all had at least some fluid-like character and could be aspirated. From measurements of vesicle and pipette diameters, membrane extension, and applied pressure, a stress–strain curve can be obtained, from which the area expansion elastic modulus was calculated.[42,43] Decreases in the CL content of the polymers led to significant decreases in the area expansion moduli (K_a), ranging from 30 dyn cm^{-1} for CT31 to 15 dyn cm^{-1} for PTS (Fig. 4a). These values are significantly lower than those that are observed for both lipid and poly(butadiene) (OB)-based vesicles (on the order of 200 and 100 dyn cm^{-1}, respectively).[2] These mechanical responses are not surprising, however, as OB has a higher T_g (approx. −20 °C) and we qualitatively noted that the PTS is markedly less viscous than OB at room temperature. Though structurally dissimilar from the high-T_g liquid crystalline polymers studied by Mabrouk and coworkers, it is interesting to note that the observed K_a's are similar.[44] Similar to the experimental findings of Mabrouk and coworkers, we find that these

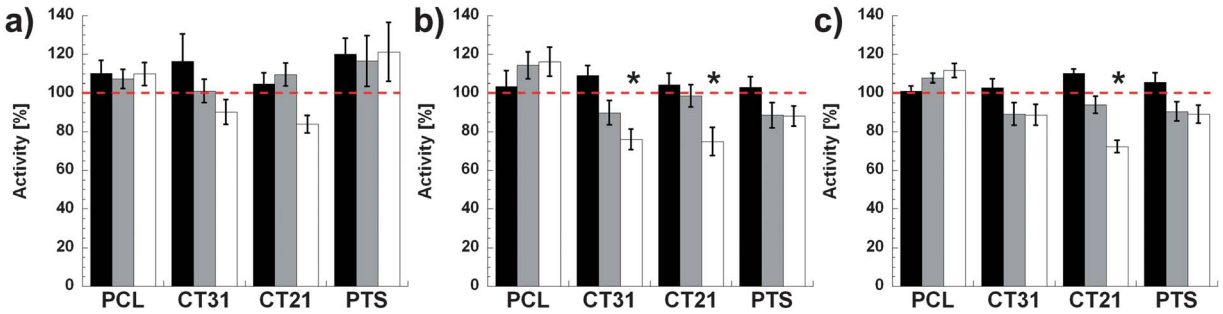

Fig. 3 Cell cytotoxicity. Metabolic activity of (a) 3T3, (b) hMSC, and (c) HUVEC cells following 24 h incubation with nano polymersomes at a concentration of 1 (black), 10 (grey) or 100 (white) μg mL^{-1} polymer. Samples normalized to polymer-free PBS controls (red lines). Data shown are means ($n = 6$) ± s.e.m. *$p < 0.05$ compared to control.

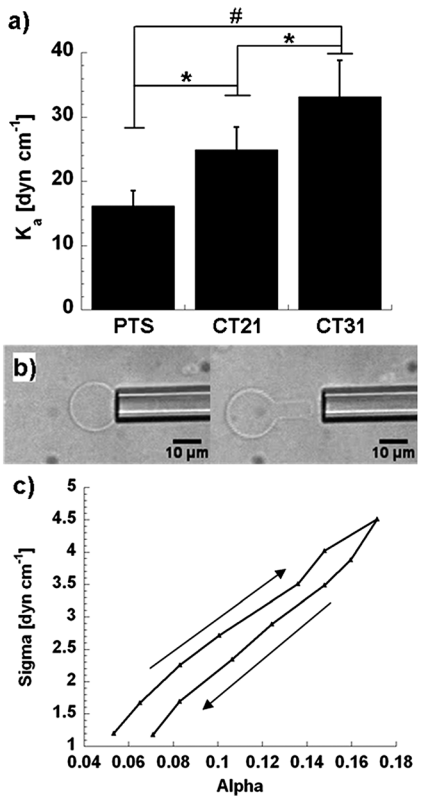

Fig. 4 Polymersome membrane characterization. (a) Apparent area expansion elastic moduli of giant vesicle membranes measured by micropipette aspiration. PCL membranes are too rigid to be aspirated. (b) A CT31 vesicle immediately before and after release from a micropipette. (c) Typical stress–strain curve for CT31 during micropipette aspiration and injection. The area expansion elastic modulus is calculated from the slope of the curve (up only). *$p < 0.0005$, #$p < 0.0001$.

vesicles, which are expected to demonstrate more solid or gel-like phase behavior, have low elastic moduli. The chemical composition or Flory–Huggins parameter of the copolymer building blocks can be more important for dictating the elastic behavior of the vesicle than the block structure and phase behavior. In accordance with this idea, we find that chemical modifications within the hydrophobic block significantly affect membrane elasticity.

We noted several interesting phenomena in our micropipette experiments that reveal information about the structure of the membrane for each composition. For most of the experiments, we were limited to a very narrow window of pipette diameter with which we could obtain extensions. Pipettes larger than ~5.7 μm in diameter aspirated entire vesicles rather than extensions, while for pipettes smaller than ~5.2 μm, extensions from vesicles often budded before they could be sufficiently aspirated. Consequently, lysis tension and critical strain could not be calculated, as no membranes failed during aspiration. Semi-permanent deformations were also observed in which CT31 and CT21 vesicles do not completely return to spheres following aspiration, but rather maintain some of their extension in their shape (Fig. 4b and S4†). This was not observed for PTS vesicles, which immediately returned to spherical morphology following release from the pipette. Probing this behavior further, we found that there was a hysteresis in the stress–strain curves of the CT31 and CT21 vesicle populations, indicating that the membranes are not purely elastic (Fig. 4c). Such deviations in elasticity could be due to the presence of nanocrystalline domains from caprolactone segments within the membrane which melt upon shearing during aspiration.[45–47] Holding the vesicle at a particular extension could allow for new nanocrystalline domains to form, allowing the vesicle to retain the aspirated shape and leading to the shape deformations observed.[46] Past reports of polymer membrane hysteresis have proposed that such behavior is due to polymer entanglements within the membrane for higher molecular weight polymers.[48] However, since such behavior is not observed for PTS vesicles whose component polymer is the same size as CT21 (and therefore would likely equally entangle), we believe that the hysteresis observed in our system is more likely caused by nanocrystalline domains acting as weak regions of polymer self-association, similar to what has been observed is model lipid systems and with erythrocytes.[42,49]

In an attempt to reduce the hysteresis and to further test our hypothesis, we repeated the micropipette aspirations of CT31 and CT21 vesicles at 30 °C, where CT21 should be in the melt state, while CT31 should remain partially crystalline (Table 1). For CT31, some hysteresis remained in the stress strain curve, though the apparent K_a of the membranes dropped to 26 dyn cm^{-1}, perhaps indicating a partial melting of the membrane. At this temperature, we found CT21 vesicles to be too soft to be able to pull reliable extensions; instead the entire vesicle aspirated into the pipette. Upon release from the pipette, the vesicles returned to their original shape. These data indicate that the CT21 vesicles are indeed fluid at this temperature (though an exact K_a cannot

be calculated) and indicate the mechanical properties of these vesicles are affected by temperature. This increasingly fluid behavior at increasing temperature further suggests that these vesicles would, indeed, exhibit ideal fluid behavior in a physiological setting.

Based on our results we are also able to estimate both the yield shear, τ_s, and surface shear viscosity, η_s, of CT membranes during aspiration. Yield shear is a measure of the shear force necessary to effect membrane flow, while the surface shear viscosity is a measure of the rate of flow into the pipette during aspiration. Descriptive equations for both have been extensively discussed by Needham and coworkers and are given as:[42,50]

$$\tau_s = [P_o R_o]/[4\ln(R_o/R_p)]$$

$$\eta_s = [\Delta P R_p^2]/[4(dL/dt)[1 - (R_p/R_o)^2]]$$

where P_o is the pressure required to draw in the membrane, R_o is the radius of the vesicle outside the pipette, R_p is the radius of the pipette, ΔP is the change in pressure, and dL/dt is the rate of change in membrane projection length. In our experiments, P_o and dL/dt were too small and rapid, respectively, to precisely measure. However, based on their qualitative assessment during micropipette aspirations, we are able to still estimate τ_s and η_s. P_o is approximately 2 cm H_2O and dL/dt is approximately 2 μm s^{-1} for a 2.5 cm H_2O change in pressure. Using typical values for R_p (5.5 μm) and vesicle radius (15 μm), τ_s and η_s are calculated to be approximately 170 dyn cm^{-1} and 1 dyn s cm^{-1}. This value for shear viscosity closely matches that which has been previously determined for poly(butadiene)-based vesicles,[51] and is several orders of magnitude lower than shear viscosity for liquid crystalline polymer membranes.[44] The value for yield shear is an order of magnitude higher than what has been observed for lipid vesicles and an order of magnitude lower than lipid particle shells.[42,50] To the best of our knowledge, yield shear has not been previously measured for polymersome systems.

While micropipette is a useful tool for probing the membrane properties of giant vesicles, it cannot be used to assess the materials properties of nano vesicles. Since nano vesicle membranes are under significantly more tension at a given transmembrane pressure than giant vesicles due to their increased curvature, we wanted to probe if the relationship between membrane elastic modulus and composition observed for giant vesicles translate to nano vesicles.[52] To probe membrane structure, we loaded the **PZn_2** fluorophore into the membranes of nano vesicles. **PZn_2** emission wavelength is highly sensitive to the chemical composition and phase behavior of the membrane, as polymer–polymer interactions within the bilayer influence the extent of **PZn_2** structural heterogeneity and the fluorophore-localized dielectric environment. **PZn_2** peak emission can thus be used as a measure of the internal environment of the membrane.[53–55] A marked increase in the **PZn_2** peak emission wavelength was observed with increasing polymer CL content (Fig. 5). This behavior is consistent with earlier data that demonstrate that increased polymer chain ordering (increased membrane crystallinity) drives decreased fluorophore structural heterogeneity resulting in more planarized **PZn_2** structures that emit at longer wavelength.[53–55] These shifts in **PZn_2** fluorescence band maxima chronicled in Fig. 5 correlate well with the thermal properties of the parent polymers and the rheological data found for giant vesicles.

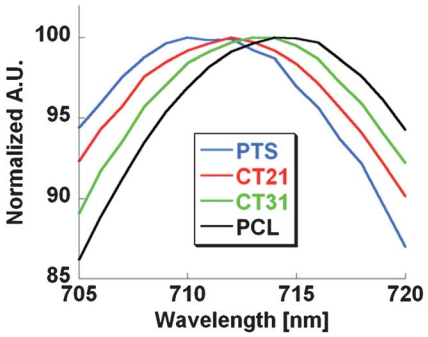

Fig. 5 Fluorescence emission spectra for **PZn_2** loaded at 2 mol% relative to polymer into nano vesicle membranes.

Membrane transport

A major benefit of using vesicles instead of micelles for drug delivery is the ability to encapsulate large quantities of hydrophilic—in addition to hydrophobic—material. When PCL vesicles were first developed, they were used to encapsulate and release doxorubicin in a controlled manner *via* transmembrane diffusion of the drug following encapsulation.[25] In the development of TOSUO-based polymersomes, there was some concern that the addition of the cyclic ketal to the membrane could alter the membrane transport (*e.g.* release) properties and lead to rapid and uncontrolled release. To address this concern, we passively encapsulated gemcitabine, a cytidine analogue used in the treatment of various cancers,[56] in the aqueous core of nano vesicles. Passive encapsulation is not ideal for many drug applications due to the poor loading efficiency, but is acceptable for our application as we aimed solely to assess the membrane transport properties of the vesicles. Following removal of unencapsulated drug by cold-temperature dialysis, release of the drug into PBS was monitored by UV absorbance for seven days (Fig. 6). All four polymers show similar first-order release profiles, releasing about 80 percent of the gemcitabine during the study. Fifty percent release is achieved after 30–48 hours, which is slightly longer than what was observed for doxorubicin release from PCL (18–24 h).[25] This release rate is still well within the time-frame required for cancer therapy, as the peak

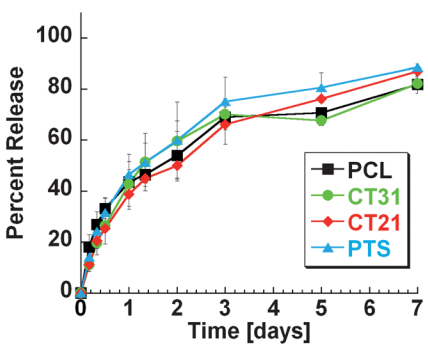

Fig. 6 Release of encapsulated gemcitabine at pH 7.4 and 37 °C from nano vesicles.

accumulation of polymersomes in tumor models appears to be around 24 hours, suggesting that these release kinetics would favor maximal accumulation of drug at the tumor site.[4] The increase in time constant is likely due to gemcitabine being more hydrophilic than doxorubicin, reducing its ability to partition across the vesicle membrane. However, similarities in the release profiles from vesicles of the four polymers indicate that the addition of TOSUO to the polymer does not significantly alter the vesicle membrane transport properties as it relates to small molecule drug release.

Experimental

Materials

Except as noted, all materials were purchased from Sigma-Aldrich and used as received. ε-Caprolactone (CL) was dried for 48 hours over calcium hydride and distilled under reduced pressure before use. *Meso*-to-*meso* ethyne-bridged (porphinato) zinc(II) dimer (**PZn_2**) was synthesized with macrocycle-pendant 10- and 20-aryl ring 3,5-(3,3,dimethyl-1-butyloxy) and 10′- and 20′-aryl ring 3,5-(9-methoxy-1,4,7-trioxanonyl) solubilizing substituents as previously reported.[6,54] Toluene was dried over calcium hydride and distilled before use. All other solvents were HPLC grade or better. Nitrogen was ultra-high purity grade and passed over Drierite before use.

Synthesis of 1,4,8-trioxaspiro-[4,6]-9-undecanone (TOSUO)

TOSUO was synthesized by the Bayer–Villager oxidation of 1,4-cyclohexanedione monoethylene acetal according to previous reports.[38,57] In a typical reaction, 21 g (134 mmol) 1,4-cyclohexanedione monoethylene acetal were dissolved in 150 mL dichloromethane, dried with magnesium sulfate, and filtered into an oven-dried 500 mL three-neck round-bottomed flask purging with nitrogen and equipped with a 250 mL addition funnel. 36 g (148 mmol) 2-chloroperoxybenzoic acid (77%) were dissolved in 200 mL dichloromethane, dried with magnesium sulfate and filtered into the addition funnel. The reaction was chilled on an ice-water bath and the 2-chloroperoxybenzoic acid solution was added drop wise over a 30 minute period. After addition, the addition funnel was removed and replaced with a condenser under nitrogen flow. The reaction was then refluxed at 40 °C for 18 hours. The reaction was chilled to 0 °C and filtered to remove the precipitate. 15 g sodium bisulfite were dissolved in 50 mL water and added to the reaction, stirring vigorously for 3 hours. 200 mL 1 M sodium bicarbonate was slowly added until no additional gas evolution was observed. The organic layer was collected, dried with magnesium sulfate, and the solvent was removed by rotary evaporation, yielding a clear oil. The crude product was twice recrystallized from dry ethyl ether under nitrogen to avoid condensation and dried under vacuum at ambient temperature. Yield: 56%. ^{1}H NMR (360 MHz, $CDCl_3$, δ): 4.3 (t, $J = 4.8$, 2H, COO–CH_2), 4.0 (s, 4H, O–CH_2), 2.7 (t, $J = 5.2$, 2H, CO–CH_2), 2.0 (t, $J = 4.8$, 2H, CH_2), 1.9 (t, $J = 5.9$, 2H, CH_2).

Synthesis of poly(ethylene glycol)-*b*-poly(TOSUO) (PTS)

PTS was synthesized by the ring-opening polymerization of TOSUO using monomethoxy-PEG as a macroinitiator and stannous octoate as the catalyst (Scheme 1). 500 mg PEG (2000 Da, 0.25 mmol) were dried under vacuum at 90 °C for 18 hours in a three-neck 100 mL round-bottomed flask before use. Following purging of the flask with nitrogen and cooling, 3.25 g (18.9 mmol) TOSUO and 3 drops of stannous octoate were added to the flask. The contents were melted and homogenized by magnetic stirring for 30 minutes at 70 °C after which the temperature was raised to 130 °C and vacuum was applied to initiate polymerization. Polymerization was allowed to proceed for 4 hours and was quenched by cooling to room temperature and dissolution of the crude polymer in THF. The catalyst was removed by addition of 1 mL of water to the still warm polymer solution. The polymer was precipitated into hexanes, dissolved in dichloromethane, and precipitated into ethyl ether. The final product was collected in dichloromethane and dried *in vacuo* overnight.

Synthesis of poly(ethylene glycol)-*b*-poly(CL-*r*-TOSUO) (PCL, CT31, CT21)

PCL, CT31, and CT21 were synthesized by the simultaneous ring-opening polymerization of CL and TOSUO (for CT31 and CT21) using monomethoxy-PEG as a macroinitiator and triethylaluminum as the catalyst (Scheme 1). In a typical reaction, 300 mg PEG were dried in a three-neck 100 mL round-bottomed flask for 18 hours at 90 °C under vacuum. Following nitrogen purge, the desired amounts of CL and TOSUO were added by syringe and pouring, respectively. The combined mass of the two monomers was held constant at 1.8 g in the reaction. 20 mL dry toluene were added to the reaction by cannula and the reactants were allowed to dissolve. Finally, 1 drop of triethyl aluminum (1.9 M in toluene) was added *via* cannula and the reaction was allowed to proceed for 18 hours at 70 °C. The reaction was quenched by the addition of 100 μL 0.1 M aqueous HCl, solubilizing the catalyst. Following removal of the toluene by rotary evaporation, the crude product was dissolved in THF and precipitated into hexanes. CT21 and CT31 were further purified by dissolution in dichloromethane and precipitation into ethyl ether. The final product was collected in dichloromethane and dried *in vacuo* overnight. PCL was redissolved in dichloromethane and precipitated into hexanes. The final polymer was collected in a Buchner funnel and dried overnight.

Polymer characterization

NMR spectra were recorded on a Bruker Avance 360 MHz spectrometer. Gel permeation chromatography (GPC) was performed on a Waters HPLC system with Styragel HR 2E and 4E columns in series. THF was used as the eluent at 0.3 mL min^{-1} at 40 °C, and the instrument was calibrated to polystyrene standards. Because of the known poor calibration between poly(styrene) standards and polyesters, molar masses as calculated by GPC are not reported.[58,59] Differential scanning calorimetry was performed on a TA Instruments Q2000 Differential Scanning Calorimeter (New Castle, DE) using aluminum sample pans. Samples were heated at 20 °C min^{-1} to 100 °C, held at that temperature for 5 min, cooled at 5 °C min^{-1} to −80 °C, and then after a 5 min isotherm, heated to 100 °C at 5 °C min^{-1}.

Vesicle assembly

Polymersomes were assembled by the rehydration method.[25] Specifically, a thin film of polymer was cast from dichloromethane onto a roughened Teflon chip and was dried for at least 24 h *in vacuo* to ensure complete solvent removal. For samples containing porphyrin, the porphyrin was co-cast with the polymer in the film. Polymersome assembly was initiated by immersion of the films in aqueous media (water, PBS or 2 vol% glycerol) and heating to 62 °C. Hydrophilic encapsulants were dissolved in the aqueous media and removed by dialysis following assembly. To assemble giant (*i.e.* > 5 μm) vesicles, the films were heated for 48–72 hours and then vortexed for 60 seconds. To assemble nano-sized vesicles, following 30 minutes of heating, the films were sonicated for 60 min at the same temperature. To minimize multilamellar vesicles, nano-sized vesicles were further subjected to 4 cycles of freezing in liquid nitrogen and thawing.

Microscopy

Confocal images of giant polymersomes were obtained on an Olympus Fluoview FV1000 confocal microscope (Center Valley, PA), equipped with a UPLFLN 40× oil objective lens. Porphyrin fluorescence images were collected by excitation with 488, 543 and 633 nm lasers with a long pass emission filter set to 650–750 nm. Scan speed was set to 2 pixels s^{-1} in Kalman mode.

Cryo transmission electron microscopy

Samples for cryoTEM were prepared in the humidity chamber of a cryoplunger (Gatan Cp3, Warrendale, PA) at 80% relative humidity. 2.5 μL of sample were deposited on lacey formvar/carbon 200 mesh grid (Ted Pella). The sample was blotted for 2 seconds with filter paper and was then plunged into liquid ethane cooled to −181 °C by liquid nitrogen. The sample was then transferred to a sample holder and stored in liquid nitrogen. The cryoholder (Gatan CT3500TR) was filled with liquid nitrogen and brought to −186 °C. The work station was filled with liquid nitrogen and the cryoholder was inserted. The sample holder was placed in the work station, a sample was transferred to the cryoholder, and the shutter was closed. The cryoholder was immediately inserted into the TEM (JEOL 2010, West Chester, PA) operating at 120 kV. After establishing a Gaussian image and making alignment adjustments, the image was underfocused by 5 μm to 15 μm for contrast. To minimize dose and reduce melting of the sample, the condenser aperture was set to 70 μm and the spot size was set to 3. Just prior to image capture the spot size was set to 1. Image capture was performed with an Orius SC200 digital camera (Gatan).

Cell cytotoxicity

Polymersomes were assessed for their potential interference with cell growth. To sterilize the polymersomes, prior to film rehydration, the films were exposed to germicidal UV for 45 min. Sterile Dulbecco's PBS (dPBS, Gibco) was used as the rehydration media and the vials were sealed to prevent contamination during vesicle formation. Three cell types were studied: 3T3 fibroblasts (ATCC), human umbilical vein endothelial cells (HUVECs, Lonza, Walkersville, MD), and human mesenchymal stem cells (hMSCs, Lonza). All cell cultures were maintained at 37 °C in a humidified incubator with 5% CO_2. 3T3s were cultured in Dulbecco's Modified Eagle Medium (Gibco) supplemented with 10% fetal bovine serum (FBS, Gibco) and 1% penicillin/streptomycin. HUVECs were maintained in endothelial growth media (Lonza) with 2% FBS (Lonza), 0.4% bovine brain extract with heparin (Lonza), 0.1% human endothelial growth factor (Lonza), and 0.1% hydrocortisone (Lonza). HUVECs were washed with HEPES-buffered saline rather than PBS. hMSCs were cultured in modified eagle medium-alpha (Gibco) supplemented with 16% FBS (Gibco), 1% L-glutamine, and 1% penicillin/streptomycin. HUVECs were used at passage 7 and hMSCs were used at passage 3. 24 hours before incubation with polymersomes, cells were plated at a density of 5000 cells per well in 96 well plates. Polymersomes or dPBS (control) were added to the cell cultures to a final concentration of 10 vol% dPBS/polymersomes in serum-containing media. After 24 hours, media was aspirated, the cells were washed with dPBS or HEPES-buffered saline, and fresh media was added. 48 hours after the addition of polymersomes, the media was replaced with a 10 vol% solution of Alamar Blue (Invitrogen) in media. The fluorescence was measured after 3.5 hours (ex/em = 540/590 nm, Tecan Infinity M200, Durham, NC). Samples were normalized to PBS controls, taken to be 100% viability.

Micropipette aspirations

Micropipettes of borosilicate glass (Friedrich and Dimmock, Milville, NJ) were prepared using a needle/pipette puller (Model 720, David Kopf Instruments, Tujunga, CA) and microforged using a glass bead to give the pipette tip a smooth, flat edge. Inner diameters of the pipettes ranged from 5.2 to 5.7 μm and were measured using a calibrated probe, optical microscopy, and computer imaging software. Following filling with 2 vol% glycerol containing 1 wt% bovine serum albumin (BSA), the pipettes were attached to an aspiration station mounted on the side of a Zeiss inverted microscope, equipped with a manometer, Validyne pressure transducer (models DP 15-32, and DP 103-14, Validyne Engineering Corp., Northridge, CA), digital pressure readouts, micromanipulators (model WR-6, Narishige, Tokyo, Japan), and MellesGriot millimanipulators (coarse *x*, *y*, *z* control). Suction pressure was applied *via* a syringe attached to the manometer. Pipettes were used to select single vesicles for aspiration. At least 10 vesicles per group were analyzed. Pressure was increased stepwise in 2.5 cm H_2O increments, and the membrane was allowed to equilibrate for at least 5 s between increments. Experiments were imaged using DIC optics with a 40× objective and a Cohu black-and-white CCD camera (Cohu, Inc., San Diego, CA). ImageJ software (National Institutes of Health, Bethesda, MD) was used to measure membrane extensions and vesicle diameters. Calculations of tension and area extension were performed using force balances described by Evans.[42,43]

Fluorescence measurements

Fluorescence measurements were made on a SPEX Fluorolog-3 fluorimeter (HORIBA Jobin Yvon, Edison, NJ). Excitation was set to 480 nm and emission was measured from 600–850 nm in

1 nm increments with a 0.1 s integration time. Experiments were performed at room temperature (approximately 23 °C).

Encapsulant release

Gemcitabine-loaded polymersomes were fabricated by assembly of the vesicles in a PBS solution of the drug (2 mg mL^{-1} Gemzar, Eli Lilly, Indianapolis, IN). Unencapsulated gemcitabine was removed *via* dialysis at 4 °C in order to inhibit release of encapsulated material. To ensure that no encapsulated material was releasing, dialysate was also measured for gemcitabine presence, which was not observed. Samples were split into 3 dialysis cassettes per polymer (SpectraPor Float-A-Lyzer G2, 50 kDa molecular weight cutoff). 600 μL sample were placed in each cassette and each cassette was placed into 60 mL PBS in a polystyrene jar (for gemcitabine). Each jar was capped and incubated at 37 °C on a rotary shaker. Aliquots (1 mL) were removed at prescribed time points and were measured for absorbance at 270 nm and returned to the sample. To calculate 100% release, after the final time point, 600 μL 1% TritonX-100 were added to each sample and the dialysis was allowed to continue for an additional hour at 37 °C, following which a final aliquot was removed and analyzed.

Statistics

Statistical significance was determined by one-way ANOVA of datasets with Tukey's post-hoc analysis using JMP software (Cary, NC). $p < 0.05$ was considered to be statistically significant.

Conclusion

Polymersomes are a promising class of materials for the development of novel theranostic carriers. Poly(caprolactone)-based carriers are of particular interest because of their biocompatibility and biodegradability. However, the applications of PEG–PCL vesicles are limited by the crystallinity of their membranes. By copolymerizing the monomer TOSUO with the caprolactone, we have developed non-toxic hydrolysable vesicles with reduced membrane crystallinity. The introduction of TOSUO has only a minor effect on polymersome transport properties and cell compatibility but provides a route to significantly alter membrane rheological properties, which have been assessed by micropipette aspiration and the emission of embedded NIR-emissive porphyrin-based fluorophores. Future work will focus on further development of TOSUO-based vesicles into clinically relevant drug delivery devices.

Acknowledgements

The authors acknowledge funding from the Penn NSF MRSEC DMR11-20901 and the Packard Foundation. J.S.K. and N.P.K were supported by Graduate Research Fellowships from the NSF. We thank Prof. Darrin Pochan and Jiahua Zhu for help with cryoTEM, Prof. Xinqiao Jia and Dr Xiaoying Wang for helpful discussions regarding TOSUO preparation, and Dr Murat Guvendiren and Dr Randi Saunders for useful discussions. ESI† is available online from RSC or from the author.

References

1 R. Langer and D. A. Tirrell, *Nature*, 2004, **428**, 487–492.
2 B. M. Discher, Y. Y. Won, D. S. Ege, J. C. M. Lee, F. S. Bates, D. E. Discher and D. A. Hammer, *Science*, 1999, **284**, 1143–1146.
3 D. E. Discher and F. Ahmed, *Annu. Rev. Biomed. Eng.*, 2006, **8**, 323–341.
4 F. Ahmed, R. I. Pakunlu, A. Brannan, F. Bates, T. Minko and D. E. Discher, *J. Controlled Release*, 2006, **116**, 150–158.
5 D. H. Levine, P. P. Ghoroghchian, J. Freudenberg, G. Zhang, M. J. Therien, M. I. Greene, D. A. Hammer and R. Murali, *Methods*, 2008, **46**, 25–32.
6 V. S.-Y. Lin, S. G. DiMagno and M. J. Therien, *Science*, 1994, **264**, 1105–1111.
7 N. A. Christian, F. Benencia, M. C. Milone, G. Li, P. R. Frail, M. J. Therien, G. Coukos and D. A. Hammer, *Mol. Imag. Biol.*, 2009, **11**, 167–177.
8 P. P. Ghoroghchian, P. R. Frail, K. Susumu, D. Blessington, A. K. Brannan, F. S. Bates, B. Chance, D. A. Hammer and M. J. Therien, *Proc. Natl. Acad. Sci. U. S. A.*, 2005, **102**, 2922–2927.
9 N. A. Christian, M. C. Milone, S. S. Ranka, G. Z. Li, P. R. Frail, K. P. Davis, F. S. Bates, M. J. Therien, P. P. Ghoroghchian, C. H. June and D. A. Hammer, *Bioconjugate Chem.*, 2007, **18**, 31–40.
10 Z. Pang, W. Lu, H. Gao, K. Hu, J. Chen, C. Zhang, X. Gao, X. Jiang and C. Zhu, *J. Controlled Release*, 2008, **128**, 120–127.
11 D. Demirgoz, T. O. Pangburn, K. P. Davis, S. Lee, F. S. Bates and E. Kokkoli, *Soft Matter*, 2009, **5**, 2011–2019.
12 G. P. Robbins, R. L. Saunders, J. B. Haun, J. Rawson, M. J. Therien and D. A. Hammer, *Langmuir*, 2010, **26**, 14089–14096.
13 G. P. Robbins, D. Lee, J. S. Katz, P. R. Frail, M. J. Therien, J. C. Crocker and D. A. Hammer, *Soft Matter*, 2011, **7**, 769–779.
14 J. A. Zupancich, F. S. Bates and M. A. Hillmyer, *Biomacromolecules*, 2009, **10**, 1554–1563.
15 J. S. Katz, D. H. Levine, K. P. Davis, F. S. Bates, D. A. Hammer and J. A. Burdick, *Langmuir*, 2009, **25**, 4429–4434.
16 N. Kamat, G. P. Robbins, J. Rawson, M. J. Therien, I. J. Dmochowski and D. A. Hammer, *Adv. Funct. Mater.*, 2010, **20**, 2588–2596.
17 E. Mabrouk, D. Cuvelier, F. Brochard-Wyart, P. Nassoy and M. H. Li, *Proc. Natl. Acad. Sci. U. S. A.*, 2009, **106**, 7294–7298.
18 G. P. Robbins, M. Jimbo, J. Swift, M. J. Therien, D. A. Hammer and I. J. Dmochowski, *J. Am. Chem. Soc.*, 2009, **131**, 3872–3874.
19 B. M. Discher, H. Bermudez, D. A. Hammer, D. E. Discher, Y. Y. Won and F. S. Bates, *J. Phys. Chem. B*, 2002, **106**, 2848–2854.
20 J. S. Katz, S. Zhong, B. G. Ricart, D. J. Pochan, D. A. Hammer and J. A. Burdick, *J. Am. Chem. Soc.*, 2010, **132**, 3654–3655.
21 E. Mabrouk, S. Bonneau, L. Jia, D. Cuvelier, M. H. Li and P. Nassoy, *Soft Matter*, 2010, **6**, 4863–4875.
22 H. Lomas, I. Canton, S. MacNeil, J. Du, S. P. Armes, A. J. Ryan, A. L. Lewis and G. Battaglia, *Adv. Mater.*, 2007, **19**, 4238–4243.
23 H. Lomas, M. Massignani, K. A. Abdullah, I. Canton, C. Lo Presti, S. MacNeil, J. Z. Du, A. Blanazs, J. Madsen, S. P. Armes, A. L. Lewis and G. Battaglia, *Faraday Discuss.*, 2008, **139**, 143–159.
24 C. Murdoch, K. J. Reeves, V. Hearnden, H. Colley, M. Massignani, I. Canton, J. Madsen, A. Blanazs, S. P. Armes, A. L. Lewis, S. MacNeil, N. J. Brown, M. H. Thornhill and G. Battaglia, *Nanomedicine*, 2010, **5**, 1025–1036.
25 P. P. Ghoroghchian, G. Z. Li, D. H. Levine, K. P. Davis, F. S. Bates, D. A. Hammer and M. J. Therien, *Macromolecules*, 2006, **39**, 1673–1675.
26 X. Q. Yang, J. J. Grailer, I. J. Rowland, A. Javadi, S. A. Hurley, D. A. Steeber and S. Q. Gong, *Biomaterials*, 2010, **31**, 9065–9073.
27 C. Sanson, C. Schatz, J. F. Le Meins, A. Brulet, A. Soum and S. Lecommandoux, *Langmuir*, 2010, **26**, 2751–2760.
28 K. Rajagopal, A. Mahmud, D. A. Christian, J. D. Pajerowski, A. E. X. Brown, S. M. Loverde and D. E. Discher, *Macromolecules*, 2010, **43**, 9736–9746.
29 J. A. Zupancich, F. S. Bates and M. A. Hillmyer, *Macromolecules*, 2006, **39**, 4286–4288.
30 M. J. Paszek, D. Boettiger, V. M. Weaver and D. A. Hammer, *PLoS Comput. Biol.*, 2009, **5**(12), e1000604.
31 T. J. English and D. A. Hammer, *Biophys. J.*, 2005, **88**, 1666–1675.
32 H. Y. Yuan, J. Li, G. Bao and S. L. Zhang, *Phys. Rev. Lett.*, 2010, **105**, 138101.

33 M. Deserno and T. Bickel, *Europhys. Lett.*, 2003, **62**, 767–773.
34 R. K. Jain, *Cancer Metastasis Rev.*, 1987, **6**, 559–593.
35 M. E. Fox, F. C. Szoka and J. M. J. Frechet, *Acc. Chem. Res.*, 2009, **42**, 1141–1151.
36 D. Tian, P. Dubois and R. Jerome, *Macromolecules*, 1997, **30**, 1947–1954.
37 D. Tian, P. Dubois and R. Jerome, *Macromolecules*, 1997, **30**, 2575–2581.
38 D. Tian, P. Dubois, C. Grandfils and R. Jerome, *Macromolecules*, 1997, **30**, 406–409.
39 X. Wang, L. A. Gurski, S. Zhong, X. Xu, D. J. Pochan, M. J. Farach-Carson and X. Jia, *J. Biomater. Sci., Polym. Ed.*, 2011, **22**, 1275–1298.
40 Y. Y. Han, J. Cui and W. Jiang, *Macromolecules*, 2008, **41**, 6239–6245.
41 F. Checot, S. Lecommandoux, H. A. Klok and Y. Gnanou, *Eur. Phys. J. E: Soft Matter Biol. Phys.*, 2003, **10**, 25–35.
42 E. Evans and D. Needham, *J. Phys. Chem.*, 1987, **91**, 4219–4228.
43 E. A. Evans, *Biophys. J.*, 1973, **13**, 941–954.
44 E. Mabrouk, D. Cuvelier, L. L. Pontani, B. Xu, D. Levy, P. Keller, F. Brochard-Wyart, P. Nassoy and M. H. Li, *Soft Matter*, 2009, **5**, 1870–1878.
45 R. G. Larson, *Rheol. Acta*, 1992, **31**, 497–520.
46 A. Lendlein and R. Langer, *Science*, 2002, **296**, 1673–1676.
47 D. Needham, T. J. McIntosh and E. Evans, *Biochemistry*, 1988, **27**, 4668–4673.
48 H. Bermudez, A. K. Brannan, D. A. Hammer, F. S. Bates and D. E. Discher, *Macromolecules*, 2002, **35**, 8203–8208.
49 R. Waugh and E. A. Evans, *Biophys. J.*, 1979, **26**, 115–131.
50 D. H. Kim, M. J. Costello, P. B. Duncan and D. Needham, *Langmuir*, 2003, **19**, 8455–8466.
51 R. Dimova, U. Seifert, B. Pouligny, S. Forster and H. G. Dobereiner, *Eur. Phys. J. E: Soft Matter Biol. Phys.*, 2002, **7**, 241–250.
52 B. L.-S. Mui, P. R. Cullis, E. A. Evans and T. D. Madden, *Biophys. J.*, 1993, **64**, 443–453.
53 P. P. Ghoroghchian, P. R. Frail, G. Z. Li, J. A. Zupancich, F. S. Bates, D. A. Hammer and M. J. Therien, *Chem. Mater.*, 2007, **19**, 1309–1318.
54 P. P. Ghoroghchian, P. R. Frail, K. Susumu, T. H. Park, S. P. Wu, H. T. Uyeda, D. A. Hammer and M. J. Therien, *J. Am. Chem. Soc.*, 2005, **127**, 15388–15390.
55 N. P. Kamat, Z. Liao, L. E. Moses, J. Rawson, M. J. Therien, I. J. Dmochowski and D. A. Hammer, *Proc. Natl. Acad. Sci. U. S. A.*, 2011, **108**, 13984–13989.
56 M. S. Aapro, C. Martin and S. Hatty, *Anti-Cancer Drugs*, 1998, **9**, 191–201.
57 C. H. Heathcock and T. W. Vongeldern, *Heterocycles*, 1987, **25**, 75–78.
58 J. Z. Du, D. P. Chen, Y. C. Wang, C. S. Xiao, Y. J. Lu, J. Wang and G. Z. Zhang, *Biomacromolecules*, 2006, **7**, 1898–1903.
59 A. Duda, Z. Florjanczyk, A. Hofman, S. Slomkowski and S. Penczek, *Macromolecules*, 1990, **23**, 1640–1646.

